Vol. 19, No. 2 (2020) 889-902
Revista Mexicana de Ingeniería Química

Optimization of the biosynthesis of gold nanoparticles using *Hypericum perforatum* and evaluation of their antimicrobial activity

Optimización de la biosíntesis de nanopartículas de oro utilizando *Hypericum perforatum* y evaluación de su actividad antimicrobiana

J.C. Serrano-Niño, C.A. Contreras-Martínez, J.R. Solís Pacheco, A. Zamudio Ojeda, B.R Aguilar Uscanga, A. Cavazos-Garduño*

Centro Universitario de Ciencias Exactas e Ingenierías, Universidad de Guadalajara; Boulevard Marcelino García Barragán 1421, 44420. Guadalajara, Jalisco. México.

Received: July 06, 2019; Accepted: November 4, 2019

Abstract

The functionality of metal nanoparticles is reported mainly in the pharmaceutical and biomedical areas. Gold nanoparticles (AuNPs) have shown numerous activities among these the microbicidal capacity, as transporters of therapeutic drugs and in the treatment of genetic diseases. The AuNPs are synthesized by physical, chemical and biological methods; the green synthesis is an eco-friendly method based on biological principles that have functional groups serving as reducing agents and stabilizers in the reaction. The objective of this work was the optimization in the conditions for AuNPs synthesis using *Hypericum perforatum* and assess the antimicrobial activity of optimal treatments obtained. The AuNPs were synthesized by the combination of biological and physical methods; characterized by FTIR, spectrophotometry, TEM and DLS; and was evaluated the antimicrobial effect of AuNPs synthesized by an experimental design using Response Surface Methodology (RSM) and at optimized conditions. The smallest particle size obtained was 44 nm, however not all AuNPs showed antimicrobial activity, the minimum inhibitory and minimum bactericidal concentrations for *B. subtilis* were 0.42 and 0.84 μg Au/mL, respectively. The information obtained presents a method of AuNPs synthesis in a fast and free of pollutants for the environment, providing an alternative to obtain antimicrobial compounds with no microbial resistance.

Keywords: gold nanoparticles, *Hypericum perforatum*, antimicrobial activity, optimized treatments.

Resumen

La funcionalidad de las nanopartículas metálicas se ha reportado principalmente en el área farmacéutica y biomédica. Las nanopartículas de oro (AuNPs) han mostrado numerosas actividades como la capacidad microbicida, transportadores de fármacos terapéuticos y en el tratamiento de enfermedades genéticas. Las AuNPs se sintetizan mediante métodos físicos, químicos y biológicos; la síntesis verde es un método amigable con el medio ambiente basado en principios biológicos con grupos funcionales actuando como agentes reductores y estabilizadores en la reacción. El objetivo de este trabajo fue la optimización en las condiciones de síntesis de AuNPs utilizando *Hypericum perforatum* y evaluar la actividad antimicrobiana de los tratamientos óptimos obtenidos. Las AuNPs se sintetizaron mediante la combinación de métodos biológicos y físicos, fueron caracterizados por FTIR, espectrofotometría, TEM y DLS, y se evaluó el efecto antimicrobiano de las AuNPs sintetizadas mediante un diseño experimental empleando la metodología de superficie de respuesta (RSM) y a condiciones optimizadas. El menor tamaño de partícula obtenido fue de 44 nm, sin embargo, no todas las AuNP mostraron actividad antimicrobiana, las concentraciones mínimas inhibitorias y bactericidas en *B. subtilis* fueron de 0.42 y 0.84 μg Au/mL, respectivamente. La información obtenida presenta un método de síntesis de AuNPs de forma rápida y libre de contaminantes para el medio ambiente, proporcionando una alternativa para obtener compuestos antimicrobianos sin resistencia microbiana.

Palabras clave: nanopartículas de oro, *Hypericum perforatum*, actividad antimicrobiana, tratamientos optimizados.

* *Corresponding author. E-mail*: adrianacavgar@gmail.com
+52 (33) 13785900-27525
https://doi.org/10.24275/rmiq/Bio790
issn-e: 2395-8472

1 Introduction

Bionanotechnology studies the influence of biological systems on the synthesis or changes towards nanostructures as well as the effects and interactions that occur between them (Vazquez-Muñoz and Huerta-Saquero, 2014). Due to its small size, the properties exhibited by nanomaterials are very different from their conventional scale, the characteristics of the nanoparticles determine the physical, chemical, optical and electronic properties and as a result their applications can be multiple in areas such as microbiology, pharmacy, ecology, industry and biomedical (Narayanan and Sakthivel, 2011). Metallic nanoparticles have specific properties that differ from those of the macro-scale metal from which they are formed, these properties show a strong dependence on size, geometry, distance between particles and the nature of the stabilizing layer (Vazquez-Muñoz and Huerta-Saquero, 2014). The synthesis methods for metallic nanoparticles are cataloged in three groups: chemical, physical and biological. Green synthesis is called the synthesis methods based on biological principles where are used plants, algae, bacteria, yeast, fungi and human cells in order to transform inorganic metal ions into metal nanoparticles via the reductive capacities of the proteins and other metabolites present in these organisms, with the advantage of employing eco-friendly compounds, safety, non toxic, and the ability to up production volumes (Abdel-Raouf *et al*., 2017; Makarov *et al*., 2014). The metal nanoparticles possibly most studied are elements such as silver, copper, iron, as well as compounds of various substances such as oxides (Makarov *et al*., 2014). Gold nanoparticles (AuNPs) are nanostructures with chemical, physical and medicinal properties, which have produced a large number of innovations with microbiological, pharmaceutical, environmental, industrial and biomedical applications (Saha *et al*., 2012; Zhang, 2015). It is important to characterize the shape, size of the nanoparticles obtained through the green synthesis by using the different biological elements and evaluating the activities (antimicrobial, thermal, reduction/degradation, among others) of the formed nanoparticles that could provide information for future applications.

The genus Hypericum ("St. John's wort") is a flowering *plant* in the family Hypericaceae, comprises nearly 500 species of shrubs, trees and herbs; more specifically *Hypericum perforatum*, known as perforate St John's-wort, is used as a medicinal herb that in recent years began to be economically important in pharmacology (Meseguer *et al*., 2013). Extracts of *Hypericum perforatum* contain at least 15 constituents or pharmacologically active components, among these are included hypericin, pseudohypericin, hyperoside, quercitrin, Isoquercitrin, quercetin, rutin, chlorogenic acid, amentoflavone, hyperforin among others; due to active compounds which are used as painkillers, antidepressants or anticancer treatments this plant has been used for the development of nutraceuticals, teas, tinctures, juices and oily macerates (Barnes *et al*., 2001; Gaedcke, 2003; Koyu and Haznedaroglu; 2015).

The antimicrobial effect of the AuNPs is of great scientific relevance due to the null capacity to form resistance by microorganisms, then the conditions for the synthesis of AuNPs were studied by a method based on the combination of biological and physical agents, which are green synthesis and exposure to microwave radiation; the extract of *Hypericum perforatum*, was selected for the formation of AuNPs, since it serves as a precursor of reducing agents in the formation reaction and together with the microwave radiation, the synthesis times are reduced to seconds. Experimental design using Response Surface methodology and the optimization have allowed to evaluate the effect of multiple factors and their interactions and performing mathematical modeling, in addition to reducing the number of samples, time and the costs of experimentation; in several works has been reported the use of this tool to obtain the process conditions for extraction of antioxidant compounds, the formation of edible antioxidant films and even in plant germination processes (De la Mora-López *et al*., 2018; Felix *et al*., 2018; López-Hernández *et al*., 2018). For the above, the aim of this work was the optimization in the conditions for AuNPs synthesis using *Hypericum perforatum* and assess the antimicrobial activity of optimal treatments obtained.

2 Materials and methods

2.1 Materials and bacterial strains

As a gold precursor was employed Gold (III) chloride trihydrate from Sigma (HAuCl4.3H2O, Sigma Aldrich, 99.9%). *Hypericum perforatum* plant was obtained from the local market in Guadalajara Jalisco,

México. The water used in the whole experiment was Milli Q type. Staphylococcus aureus, *Escherichia coli, Staphylococcus epidermidis, B. subtilis, Salmonella typhimurium* and *Listeria monocytogenes*, the strains are from ATCC collections belong to the research laboratory in industrial microbiology and were grown in soy-tripticase broth at 32 ºC on an orbital shaker at 100 rpm. All other chemicals and reagent used were of analytical grade or higher.

2.2 Preparation of the Hypericum perforatum infusion

The *Hypericum perforatum* (HP) inflorescences were used to obtain the infusion, flowers were separated from the plant and dried in oven at 50 ºC for 4 h, once dried they were milled at 30 mesh, then 1 g was mixed with 50 mL of distilled water and heated at 50 °C for 30 min without stirring. This infusion was filtered in whatman paper, then centrifuged at 5000 rpm for 5 min and finally filtered whit a syringe filter (0.4 μm) and stored at 4 °C before use it. Characterization was made by analysis of the concentration of total phenols by the colorimetric method of Folin-Ciocalteu reported by Singleton and Rossi (1965); and the antioxidant capacity by the DPPH test using the method reported by Cruzado *et al*. 2013.

2.3 Preparation and characterization of gold nanoparticles

The formation of the gold nanoparticles was carried out by a combination of green synthesis and a physical method; different volumes of the HP infusion were contacted with 4 ml of the gold solution at different concentrations (mM) and were exposed to microwave irradiation for 7 s. In order to evaluate if gold nanoparticles were formed in each treatment the characterization was carried out by UV-vis spectrophotometry, particle size analysis, Fourier Transforms Infrared Spectroscopy (FTIR) and electron microscopy. All experimental runs were performed in triplicate.

Synthesized particles obtained from the experimental design were characterized by UV-Vis spectroscopy using Thermo Scientific Genesys 10S at a resolution of 1 nM from 400 to 800 nM. FTIR analysis was used to identify the possible biomolecules responsible for the reduction of the Au ions during the biosynthesis of gold nanoparticles using an extrac of HP and determine the interactions between the components that may occur as reported in the particle synthesis (Hernández-Téllez *et al*., 2018). For particle size, particle size dispersion (polydispersity index) and surface charge (zeta potential) a Zetasizer Nano-ZS90 (Malvern Instrument Inc) was used, using the undiluted sample. For transmission electron microscopy analysis, a drop of aqueous solution containing the gold nanoparticles was placed on the carbon-coated grids. The samples were dried and kept under a desiccator; the transmission electron microscopy (TEM) measurements were performed on TESCAN model MIRA 3 LMU operating at 200 kV.

2.4 Experimental design and statistical analysis

Response surface methodology (RSM) was used to evaluate the effect of the independent variables: gold concentration (mM) and volume of *Hypericum perforatum* (HP) infusion used (μL) on the particle size obtained and inhibition zone on *E. coli*. A central composite design (CCD) was used with two factors at three levels and two axial points. The main, quadratic and the interaction effects of the independent variables on the response variables were evaluated. The design with the uncoded independent variables used is listed in Table 1. A second-order polynomial equation was used for predicting the particle size and distribution of the nanoemulsions as a function of the independent variables (Eq. 1).

$$y = \beta_0 + \beta_i X_1 + \beta_j X_2 + \beta_{ii} X_1^2 + \beta_{jj} X_2^2 + \beta_{ij} X_1 X_2 \quad (1)$$

where y is the response variable (particle size or inhibition zone), X_1 is the Gold concentration, X_2 is the volume of HP infusion used (μL), β_0 the intercept, β_i the coefficients of the first-order model, β_{ii} the quadratic coefficients for the variable i, and β_{ij} is the coefficient of the linear model for the interaction between factors i and j. The estimation that equation fits the experimental data was measured by the coefficient of determination value (R^2). The CCD was used to optimize the variables leading to a minimum particle size and a high inhibition zone value using the optimization tool of the statistical software. The experimental design matrix, data analysis, optimization procedure was performed using the statistical software package MINITAB v. 17.0.

2.5 Evaluation of the antimicrobial effect

2.5.1 Well diffusion method

The antimicrobial effect was evaluated using the well diffusion method on Mueller-Hinton agar. The bacteria used were *Staphylococcus aureus, Escherichia coli, Staphylococcus epidermidis, Bacillus subtilis, Salmonella typhimurium* and *Listeria monocytogenes*. The fresh culture of each microorganism was inoculated in tryptic soy broth and incubated at 32 °C for 18 h.

The bacterial suspension was prepared with a turbidity of the 0.5 McFarland (McF) scale and plated on Mueller-Hinton agar plates. The wells were filled with 80 μl of samples of experimental design treatments or the optimal treatments obtained and subsequently incubated at 32 °C for 8 h. All tests were performed in triplicate. After the incubation period, the diameter of the inhibition zones was measured. Statistically significant differences between the means of groups were assessed by using one-way ANOVA and Tukey's test ($p < 0.05$) carried out Minitab 18 (Minitab, Inc., State College, PA).

2.5.2 Determination of minimum inhibitory concentration (MIC)

The minimum inhibitory concentration (MIC) was evaluated in four bacterial strains: *Staphylococcus aureus, Escherichia coli, Bacillus subtilis* and *Salmonella typhimurium*, concentrations ranging from 0.43 to 50 μg AuNPs/mL were tested. Solutions with the nanoparticles to the different concentrations were put into sterile flasks containing 15 mL of nutrient broth, then 5 mL of freshly prepared bacterial suspension (0.5 McF) was added and the culture media was incubated for 24 h at 37 °C and 120 rpm. The concentration at which no visual growth was presented was considered as the minimum inhibitory concentration (MIC). A control with distilled and sterile wáter was used instead of AuNPs.

2.5.3 Estimation of minimum bactericidal concentration (MBC)

The minimum bactericidal concentration (MBC) was determined from the batch culture studies done for the measurement of MIC values. The flasks with little or no bacterial growth were selected and plated on fresh solid media (nutrient agar) and incubated at 37 °C for 24 h. The nanoparticle concentration causing a bactericidal effect was selected based on the absence of colonies on the agar plate and was considered as the MBC. Each experiment was done in triplicate.

3 Results and discussion

3.1 Characterization of the Hypericum perforatum (HP) infusion

The HP infusion after the filtration process showed a solid content of 7.8 g/L, within the reported compounds being present in HP extracts are naphthoadiantrones, flavonoids and biflavonoids, which provide biological activity; among these are mostly pseudohypericin and hypericin components that have shown pharmacological activity, antioxidative properties and others (Orčić, *et al*., 2011; Wagner and Bladt, 1994). The concentration of total phenols was 5.06 ± 0.192 μg of gallic acid equivalents/mL of aqueous extract corresponding to 253 μg of gallic acid equivalents/ g of dry plant, this value was higher than reported for *Hypericum scabrum* (41.1 μg of gallic acid equivalents/ g of dry plant), this difference has already been reported for other plant sources of polyphenols and may be due to variations between species, environmental factors that can influence phenolic metabolism such as weather conditions, light intensity, heat, droughts (Franco-Bañuelos, *et al*., 2017), however was lower than the value found for apple bagasse residue or the antioxidant compounds of mexican oregano extracted using response surface methodologies (Felix *et al*., 2018; Flores-Martínez *et al*., 2016). Respect to antioxidant activity, the HP infusion shows ability to scavenge DPPH radicals with IC50 values of 134.38 μg/mL; in a study made by Orčić *et al*., 2011, they reported IC50 values of 1.86 - 32.4 μg/mL, the biggest antioxidant activity corresponds to chromatography fractions with flavonoids and phenolic acids, other reports mention variations in concentrations for the *H. scabrum* from 1.19 to 600 μg/mL (Heshmati, *et al*., 2018; Jiang *et al*., 2015).

3.2 Application of the experimental design and evaluation of parameters affecting the synthesis of gold nanoparticles

The experimental design allowed to observe the behavior of the variables: Gold concentration and the volume of HP infusion used; the experimental responses obtained are showed in table 1.

Table 1. Conditions evaluated in the Experimental Design for the synthesis of nanoparticles and the responses obtained.

Experiment	Factors		Particle size (nm)	Inhibition zone* (mm)
	Gold (mM)	HP infusion (μL)		
1	1.6	61	169.6 ± 9.00	15.5 ±0.58
2	4.4	61	134.2 ± 14.38	16.3 ± 3.21
3	1.6	259	67.5 ± 2.14	6 ± 0
4	4.4	259	328.8 ± 27.51	16 ± 0
5	1	160	64.6 ± 2.13	0 ± 0
6	5	160	198.5 ± 7.03	19.7 ± 0.58
7	3	20	114.4 ± 17.07	16.3 ± 3.21
8	3	300	231.0 ± 28.50	15 ± 0
9	3	160	169.8 ± 9.79	15 ± 0
10	3	160	168.9 ± 5.53	15 ± 0
11	3	160	174.4 ± 9.78	15 ± 0
12	3	160	162.9 ± 9.01	15 ± 0
13	3	160	172.1 ± 1.65	15 ± 0

*Inhibition zone evaluated on *E. coli*. Each value represents the mean ± standard deviations (SD) (n = 3).

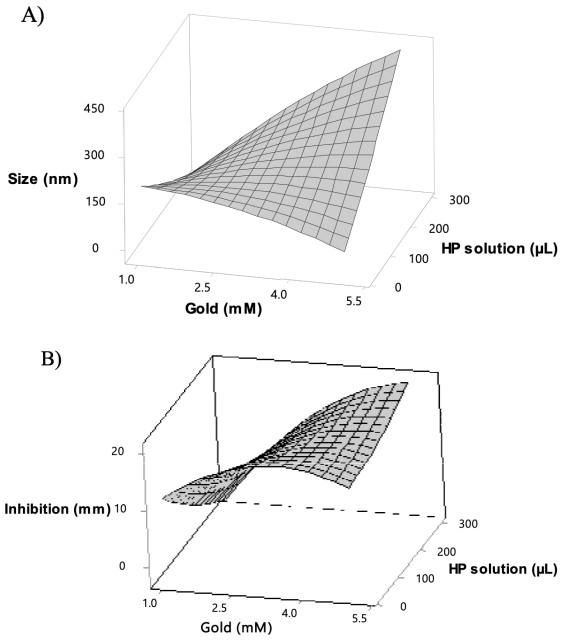

Fig. 1. Response surface plots for gold particle size (A) and for inhibition zone (B) as a function of gold concentration and the volume of HP infusion.

According to the results obtained from the experimental treatments carried out, it should be noted that the smallest size obtained was 65 nm when the gold concentration of 1 mM was used, this agrees with other studies where similar metal concentrations are used (Farah *et al*., 2016; Huang *et al*., 2007; Rajeshkumar *et al*., 2016); higher concentrations of the metal (3 to 5 mM) lead to an increase in particle size and it seems that the inhibition of microbial growth also increases.

The effect of the volume of HP infusion and the gold concentration on the particle size obtained is showed in figure 1A, for gold concentrations lower than 2.1 mM an increasing of the HP infusion causes a reduction of the particle size, according to the results obtained from the response surface methodology AuNPs with sizes of 20 nm could be obtained using 291 μL of HP infusion and a gold concentration of 1.26 mM, this due to the increase in the concentration of reducing agent present the HP infusion, above to 2.5 mM of Gold, the particle size increases when increase the volume of HP infusion, this behavior is explained as a destabilization process, where a decrease in the size of the particle, making it unstable and causing the union with other particles and an increase in size, besides this, metal ions bind to reducing agents and are reduced from Au^{+3} to Au^{0}, increasing the concentration of the reducing agent possibly by increases the amount of Au^{0}, so there are more ions with zero charge which can coalesce. This can also be corroborated by the polydispersity index (PDI), under these conditions PDI values above 0.5 were obtained.

Table 2. Regression Coefficients Describing the Influence of Variables on the particle size of AuNPs and Inhibition zone on *E. coli*.

Variable	Coefficient		Value-p	
	Particle size	Inhibition zone	Particle size	Inhibition zone
I	220.9	5.53	0	0
X_1	-8.2	7.99	0	0.001
X_2	-1.501	-0.0807	0.001	0.15
$X_1 * X_1$	-6.65	-1.203	0.073	0.041
$X_2 * X_2$	0.000741	0.000051	0.289	0.618
$X_1 * X_2$	0.5298	0.01652	0	0.112

Abbreviations: I: intercept, X_1: Gold concentration, X_2: Volume of HP infusion used. The factor is significant at the α= 0.05 level.

When using volumes less than 100 μL of HP infusion and the gold concentration increases (above 4 mM), the particle size decreases, obtaining particles with size close to 50 nm, possibly due to an adequate concentration of reducing agents to reduce chloraugic acid without reaching destabilization. The formation of nanoparticles with the smallest size was achieved at low concentrations of gold and high volumes of HP infusion.

In other works, have been reported metal concentrations around 1 nM for the nanoparticle synthesis and volumes of the solutions containing the reducing agent have been used around 1 to 30 mL, this variability in the concentrations of the metal to be reduced and the reducing agent does not allow proper conditions for the synthesis of metal nanoparticles and even to know the behavior when modifying the synthesis variables, the surface response method allowed observing the behavior at different conditions and furthermore, by means of the equation it is possible predict results at different conditions (Chandrasekaran *et al*., 2016; El-Refai *et al*., 2018; Farah *et al*., 2016; Huang *et al*., 2007; Rajeshkumar *et al*., 2016).

The regression coefficients of the model and probability values for the response variable particle size are listed in Table 2 and the Eq. 2 shows the coefficients for the particle size prediction. Negative significant effects are found in linear terms for volume of HP infusion and Gold concentration; the responses fitted to the factors in a good way with a coefficient of determination (R^2) of 96.5%.

$$\textit{Particle size} : 220.9 - 8.2X_1 - 1.501X_2 - 6.65X_1 * X_1 + 0.000741X_2 * X_2 + 0.5298X_1 * X_2 \quad (2)$$

We also evaluated the effect of independent variables on the degree of bacterial inhibition in *E. coli*, Figure 1B shows the behavior obtained, the greatest inhibition zone obtained experimentally was at the highest concentrations of gold and Volume of HP infusion used, at these conditions the larger particle sizes were obtained; so it can be thought that the inhibitory effect of the treatments is mediated more by the concentration of gold than by the size of the particle, this behavior is possibly due to the fact that the methodology of the method of diffusion of wells is being used, where a fixed amount of each treatment (80 μL) is added and the gold concentration is not adjusted to a specific value in all the treatments evaluated. In the conditions where the smallest gold particles were obtained by using low concentrations of gold, the degree of inhibition was minimal; comparing the same particle sizes with those obtained using larger gold concentrations, a difference in inhibition can be observed, in this case, a smaller particle size does not guarantee a greater activity per contact area, but the concentration of gold present in the well does. The equation obtained from the CCD for the prediction of the inhibition zone is as follows:

$$\textit{Inhibition zone} : 5.53 + 7.99X_1 - 0.0807X_2 - 1.203X_1 * X_1 + 0.000051X_2 * X_2 + 0.01652X_1 * X_2 \quad (3)$$

Of the evaluated coefficients for the inhibition zone (Table 2) only gold concentration showed a linear and quadratic significant effects on the inhibition zone; the volume of HP infusion and the interaction did not show significant effect; this corroborates that the HP infusion does not show antimicrobial activity, as evaluated in experimental previous inhibition tests; the responses fitted to the factors with a coefficient of determination (R^2) of 85%.

Table 3. Conditions for the preparation of optimal treatments.

Treatment	Gold (mM)	HP infusion μL	Particle size (nm)	PDI	Zeta potential (mV)
Optimal 1 (O1)	1.26	291	44.12 ± 1.47	0.46 ± 0.02	0.1458 ± 0.027
Optimal 2 (O2)	4.56	20	81.56 ± 1.18	0.35 ± 0.04	-0.1207 ± 0.036
Optimal 3 (O3)	5	300	410.80 ± 8.53	0.89 ± 0.09	-0.1645 ± 0.062

Each value represents the mean ± standard deviations (SD) (n = 3).

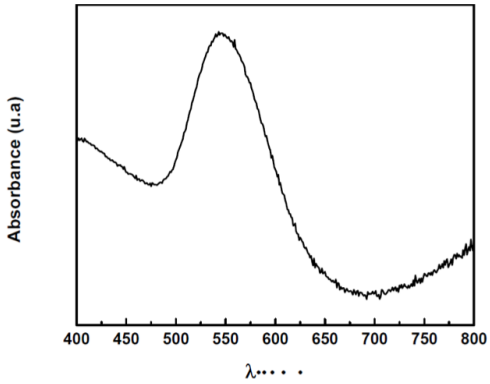

Fig. 2. UV-vis spectra of the gold nanoparticles synthesized using the HP infusion.

3.3 Optimization of the synthesis of gold nanoparticles

With the experimental results of the response surface methodology and using the Minitab 17 statistical package, it was possible to find optimal conditions that guarantee the smallest particle size (Optimal 1; particle size predicted: 20 nm), the highest inhibition (Optimal 3; Inhibition zone predicted: 20.6 mm) and a midpoint where the size and a good value of bacterial inhibition was obtained (Optimal 2; particle size predicted: 64 nm and inhibition zone predicted: 16.9 mm). As a result, three optimal conditions were obtained, the conditions for the formation of these nanoparticles are showed in Table 3. The treatments were characterized in terms of size, PDI and zeta potential.

As expected in the optimization, the O1 treatment has the smallest particle size, for the O1 treatment when specifying the reduction in particle size, the inhibition capacity that the treatment could have is not taken into account, however, if the equation for inhibition (Eq 3) was applied at the conditions of O1 treatment then the calculated value of inhibition zone was 0.57 mm, so the O1 treatment developed to obtain the smallest particle size, possibly will not show inhibition according to the results of the equation 3. For the O3 treatment, the size obtained experimentally is very close to that predicted Eq 2 (425nm), the same applies to inhibition zones around 20 mm predicted in Ec 3; the O2 treatment was designed with the purpose of combining the nanometric size and antimicrobial activity, in terms of the size this is less than 100 nanometers and has antimicrobial activity.

The zeta potential was also measured, which is the quantification of the surface charge of the particle, the values in all treatments were very close to zero, these results are in agree with the reduction of the Au^{+3} ions, where in addition to obtaining gold particles at nanometric size, the change in charge to Au^0 occurs. Sometimes the antimicrobial effect is related to the particle size and its surface charge, interactions of the particle with the cell wall and cell membrane may be mediated by the effect of the charge and the inhibition of microbial growth can occurs, in this experiment the smaller the particle size, the surface charge tends to be closer to zero, then it can be concluded that the inhibitory effect responds more to the concentration of gold used in the synthesis of AuNPs (Wang *et al*., 2017).

3.4 Characterization of gold nanoparticles

The synthesis of AuNPs has been elucidated by scanning the UV-Vis spectra, particles were scanned spectrophotometrically at a wavelength of 400 to 800 nm (Figure 2), and it was possible to observe maximum absorption with a very sharp peak around 540 nm, characteristic wavelength of the spectrum for gold nanoparticles, this is a structural characterization where the reduction of Au^{3+} ions and the formation of gold nanoparticles is confirmed; Abdel-Raouf an coworkers in 2017, reported similar results, where they have made green synthesis and obtained nanoparticles with a maximum absorbance at 536 nm. Regarding to the mechanism of synthesis of AuNPs using the infusion of HP, it is known that in HP extracts are present compounds such as naphthoadiantrones (mainly hypericin), xanthones and flavonoids which exhibit antioxidant properties, and have been attributed in others studies that are

responsible for the reduction and stabilization of silver, copper, iron, zinc and in this case gold ions for synthesis of metal nanoparticles (Rusalepp *et al*., 2017; Bunghez *et al*., 2012; El-Refai *et al*., 2018; Kuppusamy *et al*., 2016).

In order to evaluate the functional groups on HP extract and their possible relationship in the synthesis of gold nanoparticles, the FTIR analysis was carried out. The HP extract was used as control of the presence of functional groups for the synthesis of the nanoparticles, in figure 3A the presence of numerous absorption zones at frequencies lower than 1500 cm^{-1} are observed, these, form part of the own footprint of the extract and which is absent in the spectrum of the synthesized nanoparticles (figure 3B), due to this, the participation of these functional groups in biosynthesis is evidenced. The complex nature of the HP infusion is confirmed in figure 3A, the FTIR spectrum shows bans around 2170, 2000, 1730, 1530, 1320, 1150, 900- 860 cm^{-1}; the band at 1730 cm^{-1} is reported for C=O vibrations in hypericin and hyperforin (Taraj *et al*., 2019) and at 1530 cm^{-1} is from N-H vibrarion in the amide II linkages of proteins (Rajan *et al*., 2017); the band 1320 cm^{-1} can be ascribed to aromatic amines (Otari *et al*., 2015), however, it has been reported that other components present in HP extracts, germacrene and cariophyllene are found in the regions of 1460 cm^{-1} and 1377 cm^{-1} respectively (Taraj *et al*., 2019); other peaks are evident and is related to the presence of polysaccharides in the band at 1150 cm^{-1} (Rajan *et al*., 2014); the common bands for the extract and the nanoparticles are around 2170 - 2000 and 760 cm^{-1} corresponding to amides present in proteins and phenolic compund; however the intensity of bands in AuNPs decrease indicating their participation in the reduction of ions, similar behaviors have been previously reported, where the presence of these functional groups has been related to the stabilization of metallic nanoparticles (Rajan *et al*., 2017; Abdel-Raouf *et al*., 2017; Bogireddy *et al*., 2018).

The analysis of the particle size distribution of the optimal treatments (figure 4 A) shows the bimodal behavior for the O1 treatment, with marked distributions around 10 nm and 70 nm; for the O3 treatment, the behavior is multimodal with a maximum peak around 200 nm and is related to the high value of PDI. The shape and size of gold nanoparticles can be apreciated by TEM images (figure 4B), The majority of nanoparticles have sizes less than 100 nm with a spherical structure and polydisperse.

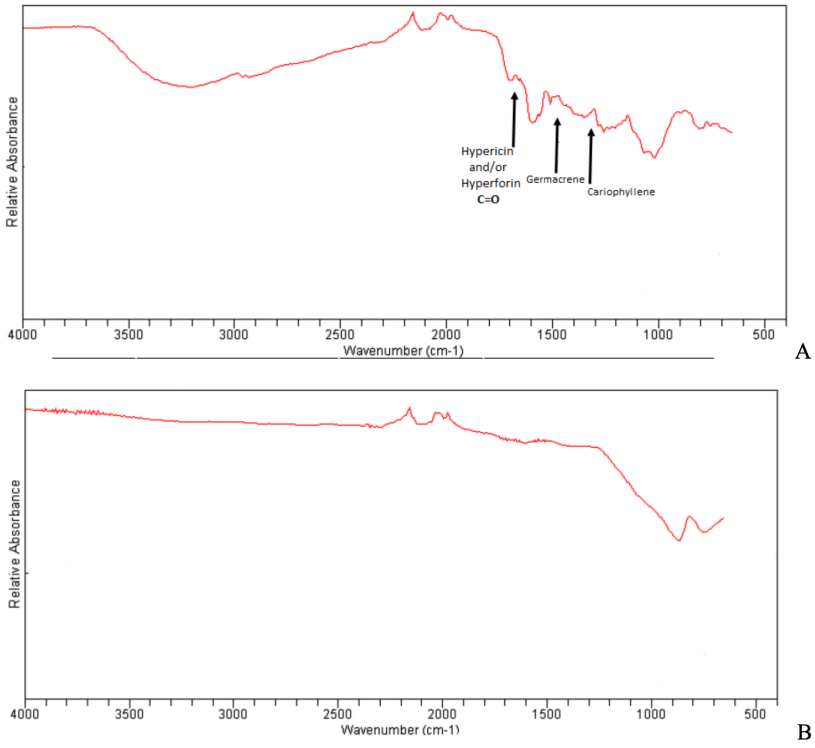

Fig. 3. FT-IR spectrum of tha HP infusión (A) and gold nanoparticles synthesized using the HP infusion at the conditions of the optimal treatment 2 (B).

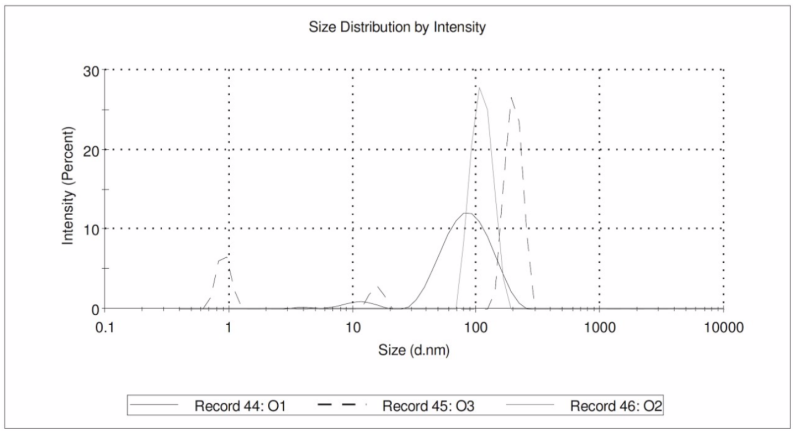

(A)

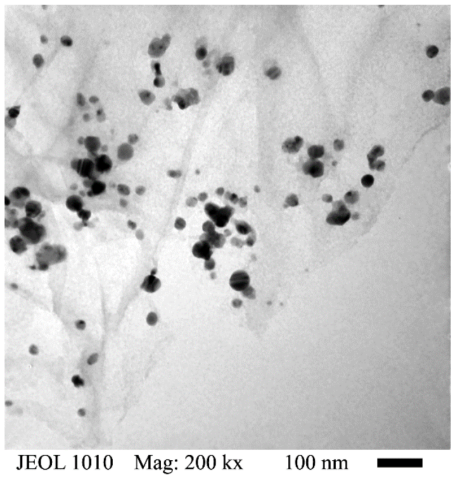

(B)

Fig. 4. Characterization of nanoparticles in optimal treatments. (A) Particle size distribution and (B) TEM image of treatmen O2.

3.5 Evaluation of the antimicrobial effect

3.5.1 Well diffusion method

The optimal treatment O1 showed no antimicrobial effect in all bacterial strains analyzed, this treatment was designed with the aim of obtaining the smallest particle size and the antimicrobial effect was not taken into account, using the equation for inhibition zone (Eq 3) at the O1 conditions, the inhibition zone calculated is 0.53 mm, it is possible that the gold concentration influenced the antimicrobial effect using the well diffusion method. On the other hand, O2 and O3 treatments have an inhibitory effect on all strains, showing inhibition zones above 14 mm (figure 5). Only with *L. monocytogenes* and *S. typhimurium* there was a significant difference ($p < 0.05$), where O3 obtained the zone of greatest inhibition (20 mm); it should be noted that the O3 treatment was designed in order to obtain the greatest inhibitory effect and the O2 treatment was designed with the purpose of combining small particle size and the inhibitory effect. In other works where the green synthesis of gold and metal nanoparticles have been carried out, inhibition zones of 17 mm or less have been reported, even by adding larger amounts of the gold nanoparticle solution. For *S. aureus*, inhibition zones close to 13.5 mm have been reported, in this work 16 mm for O3 without significant statistical difference with O2 were obtained, so we can have the antimicrobial effect in both treatments, but with the advantage of the size at the nanoscale that was initially planned for size optimization and inhibition for the O2 treatment, it is an optional feature for other applications related to particle size (Roy *et al*., 2015; Rajan *et al*., 2017; Abdel-Raouf *et al*., 2017).

Table 4. Minimum inhibitory concentration and minimum bactericidal concentration of O2 and O3 on Gram negative and Gram positive bacteria.

Minimum inhibitory concentration								
Concentration (μg Au/mL)	Gram negative				Gram positive			
	E. coli		*S. typhimurium*		*B. subtilis*		*S. aureus*	
	O2	O3	O2	O3	O2	O3	O2	O3
50	-	-	-	-	-	-	-	-
25	-	-	-	-	-	-	-	-
12.5	-	-	-	-	-	-	-	-
6.25	-	-	-	-	-	-	-	-
3.38	+	-	+	+	-	-	+	-
1.68	+	+	+	+	+	-	+	+
0.84	+	+	+	+	+	-	+	+
0.42	+	+	+	+	+	-	+	+
Minimum bactericidal concentration								
Concentration (μg Au/mL)	Gram negative				Gram positive			
	E. coli		*S. typhimurium*		*B. subtilis*		*S. aureus*	
	O2	O3	O2	O3	O2	O3	O2	O3
50	-	-	-	-	-	-	-	-
25	-	-	+	-	-	-	-	-
12.5	-	-	+	+	-	-	-	-
6.25	+	+	+	+	+	-	+	+
3.38	+	+	+	+	+	-	+	+
1.68	+	+	+	+	+	-	+	+
0.84	+	+	+	+	+	-	+	+
0.42	+	+	+	+	+	+	+	+

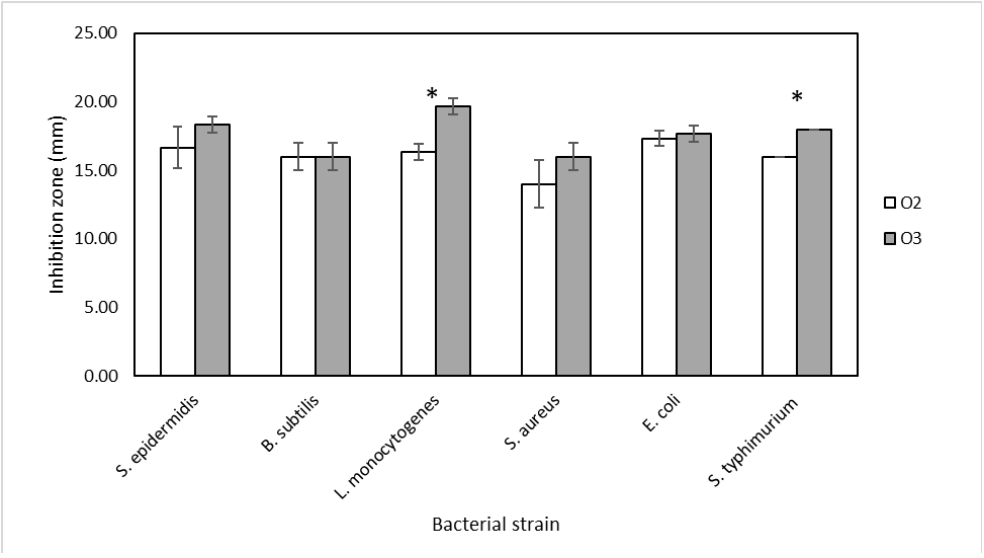

Fig. 5. Zones of inhibition in different bacterial strains obtained with the optimal treatments. * Indicates significant differences between O2 and O3 ($p < 0.05$),

3.5.2 *Determination of minimum inhibitory concentration (MIC) and minimum bactericidal concentration (MBC)*

The results are showed in terms of positive (+) and negative (-) symbols, that represents for negative no growth and growth of bacteria for positive symbol. Gold nanoparticles showed variable MIC value, however, in most cases O3 showed inhibitions at lower concentrations than O2 (Table 3). Using the O2 in the treatments with *E. coli, S. typhimurium* and *S. aureus*, the MIC value was 6.25 μg/mL and for *B. subtilis* it was 3.38 μg/mL. The MIC value of O3 in most of the bacterial strains was lower than with O2, so the objective of the optimization has an effect on the antimicrobial activity in O3. The MIC value for O3 in *S. typhimurium* was in equal concentration to O2 (6.25 μg/mL); however, for *B. subtilis* MIC value was obtained at the lowest concentration, similar results for this strain were reported by Roy et al, (2015), where the MIC value in spherical metallic nanoparticles was 0.4 μg/mL and for structures called as flower shape was 0.1 μg/mL.

The MBC value for *E. coli* and *S. aureus* was equal in O2 and O3 (12.5 μg/mL), for strains *S. typhimurium* and *B. subtilis* O3 required lower concentration (Table 3). The O2 treatment in *S. typhimurium* required the highest concentration to achieve a bactericidal effect compared to the other strains evaluated, the MBC was 50 μg/mL for O2; for *E. coli*, *S. aureus* and *B. subtilis* was the same (12.5 μg/mL). Different antimicrobial activities were observed with the O3 treatment; *Salmonella* required a high concentration (25 μg/mL) compared to *E. coli* and was 12.5 μg/mL. The value of MBC with *B. subtilis* bacteria with O3 treatment was 0.84 μg/mL. Treatment O3 was designed to show the greatest inhibitory effect and in these tests showed the lowest values of MIB and MBC, with concentrations lower than 1 μg/mL to be sufficient to kill the bacteria.

Conclusions

The use of an extract of *Hypericum perforatum* (HP) provided the reducing and stabilizing compounds for the synthesis of nano-scale gold particles and is a free alternative of hazardous or toxic materials, such as when biological methods are used. It also represents an option for the application of HP in other areas, since its use is currently in the pharmaceutical and food area due to the pharmacological effects of bioactive compounds that have already been extensively reported. The use of the HP extract as a biocatalyst coupled with the microwave-assisted method is an advantage, since the synthesis is performed in less time (less than 10 seconds) compared to other methods where the synthesis is performed using UV radiation (for minutes) or even hours when performed only by the biological method. Several biological methods for green synthesis have been reported, however, this study reports a reproducible method for obtaining nanoparticles with specific size and antimicrobial activity. With the optimal treatments, it was possible to demonstrate that the formation variables exert great effect on the characteristics of the obtained nanoparticles, besides that the size of the nanoparticles plays a important role on their antibacterial activity and the possible scope in terms of applications in different areas. The antimicrobial activity of gold nanoparticles has been in discussion due to numerous reports that relate this activity to toxic chemicals not completely removed from AuNPs, however, in this study, nanoparticles with different characteristics (mainly in terms of size) have been synthesized using safe precursor compounds presents in HP that have allowed to observe the variability in its antimicrobial activity at the synthesis conditions used.

Acknowledgements

This work was supported by PROMEP from Mexico and the Universidad de Guadalajara, we thank for the financial support for the development of this research work.

Nomenclature

HP	*Hypericum perforatum*
PDI	Polydispersity index

References

Abdel-Raouf, N., Al-Enazi, N. M., & Ibraheem, I. B. (2017). Green biosynthesis of gold nanoparticles using *Galaxaura elongata* and characterization of their antibacterial activity. *Arabian Journal of Chemistry 10*, S3029-S3039.

Barnes, J., Anderson, L. A., & Phillipson, J. D. (2001). St John's wort (*Hypericum perforatum*

L.): a review of its chemistry, pharmacology and clinical properties. *Journal of Pharmacy and Pharmacology 53*, 583-600.

Bogireddy, N. K. R., Pal, U., Gomez, L. M., & Agarwal, V. (2018). Size controlled green synthesis of gold nanoparticles using Coffea arabica seed extract and their catalytic performance in 4-nitrophenol reduction. *RSC Advances 8*, 24819-24826.

Bunghez, I. R., Barbinta Patrascu, M. E., Badea, N. M., Doncea, S. M., Popescu, A., & Ion, R. M. (2012). Antioxidant silver nanoparticles green synthesized using ornamental plants. *Journal of Optoelectronics and Advanced Materials 14*, 1016.

Chandrasekaran, R., Gnanasekar, S., Seetharaman, P., Keppanan, R., Arockiaswamy, W., & Sivaperumal, S. (2016). Formulation of *Carica papaya* latex-functionalized silver nanoparticles for its improved antibacterial and anticancer applications. *Journal of Molecular Liquids 219*, 232-238.

Cruzado, M., Pastor, A., Castro, N., Cedrón, J. C. (2013). Determinación de compuestos fenólicos y actividad antioxidante de extractos de alcachofa. *Revista de la Sociedad Química del Perú 79*, 56-63.

De la Mora-López, G. S., López-Cervantes, J., Gutiérrez-Dorado, R., Cuevas-Rodríguez, E. O., Milán-Carrillo, J., Sánchez-Machado, D. I., & Reyes-Moreno, C. (2018). Effect of optimal germination conditions on antioxidant activity, phenolic content and fatty acids and amino acids profiles of *Moringa oleifera* seeds. *Revista Mexicana de Ingeniería Química 17*, 547-560.

El-Refai, A. A., Ghoniem, G. A., El-Khateeb, A. Y., & Hassaan, M. M. (2018). Eco-friendly synthesis of metal nanoparticles using ginger and garlic extracts as biocompatible novel antioxidant and antimicrobial agents. *Journal of Nanostructure in Chemistry 8*, 71-81.

Farah, M. A., Ali, M. A., Chen, S. M., Li, Y., Al-Hemaid, F. M., Abou-Tarboush, F. M., ... & Lee, J. (2016). Silver nanoparticles synthesized from Adenium obesum leaf extract induced DNA damage, apoptosis and autophagy via generation of reactive oxygen species. *Colloids and Surfaces B: Biointerfaces 141*, 158-169.

Felix, A. C. S., Alvarez, L. D. G., Santana, R. A., Valasques-Junior, G. L., Bezerra, M. D. A., de Oliveira Neto, N. M., ... & do Nascimento Junior, B. B. (2018). Application of experimental designs for evaluate the total phenolics content and antioxidant activity of cashew apple bagasse. *Revista Mexicana de Ingeniería Química 17*, 165-175.

Flores-Martinez, H., Leon-Campos, C., Estarron-Espinosa, M., & Orozco-Avila, I. (2016). Process optimization for the extraction of antioxidants from mexican oregano (*Lippia graveolens* HBK) by the response surface methodology (RSM) approach. *Revista Mexicana de Ingeniería Química 15*, 773-785.

Franco-Bañuelos, A., Contreras-Martínez, C. S., Carranza-Téllez, J., & Carranza-Concha, J. (2017). Total phenolic content and antioxidant capacity of non-native wine grapes grown in Zacatecas, Mexico. *Agrociencia 51*, 661-671.

Gaedcke, F. (2003). St John's wort herb extracts: Manufacturing, standardisation and characterisation. In: *Hypericum* (pp. 62-77). CRC Press.

Hernández-Téllez, C. N., Cortez-Rocha, M. O., Hernández, A. B., Rosas-Burgos, E. C., Lizardi-Mendoza, J., Torres-Arreola, W., ... & Plascencia-Jatomea, M. (2018). Partículas de quitosano/carragenina/lisozima: Síntesis, caracterización y actividad antifúngica contra *Aspergillus parasiticus*. *Revista Mexicana de Ingeniería Química 17*, 897-912.

Heshmati, A., Alikhani, M.Y., Godarzi, M., & Sadeghimanesh, M. (2018). The evaluation of antioxidant and antimicrobial activities of essential oil and aqueous, methanol, ethanol, ethyl acetate and acetone extract of *Hypericum scabrum*. *International Scholarly and Scientific Research & Innovation 12*, 47 - 51

Huang, J., Li, Q., Sun, D., Lu, Y., Su, Y., Yang, X., ... & Hong, J. (2007). Biosynthesis of silver and gold nanoparticles by novel sundried *Cinnamomum camphora* leaf. *Nanotechnology 18*, 105104.

Jiang, L., Numonov, S., Bobakulov, K., Qureshi, M., Zhao, H., & Aisa, H. (2015). Phytochemical profiling and evaluation of pharmacological

activities of *Hypericum scabrum* L. *Molecules 20*, 11257-11271.

Koyu, H., & Haznedaroglu, M. Z. (2015). Investigation of impact of storage conditions on *Hypericum perforatum* L. dried total extract. *Journal of Food and Drug Analysis 23*, 545-551.

Kuppusamy, P., Yusoff, M. M., Maniam, G. P., & Govindan, N. (2016). Biosynthesis of metallic nanoparticles using plant derivatives and their new avenues in pharmacological applications-An updated report. *Saudi Pharmaceutical Journal 24*, 473-484.

López-Hernández, L. H., Calderón-Oliver, M., Soriano-Santos, J., Severiano-Pérez, P., Escalona-Buendía, H. B., & Ponce-Alquicira, E. (2018). Development and antioxidant stability of edible films supplemented with a tamarind seed extract. *Revista Mexicana de Ingeniería Química 17*, 975-987.

Makarov, V. V., Love, A. J., Sinitsyna, O. V., Makarova, S. S., Yaminsky, I. V., Taliansky, M. E., & Kalinina, N. O. (2014). "Green" nanotechnologies: synthesis of metal nanoparticles using plants. *Acta Naturae 6*, 35-44.

Meseguer, A. S., Aldasoro, J. J., & Sanmartín, I. (2013). Bayesian inference of phylogeny, morphology and range evolution reveals a complex evolutionary history in St. John's wort (Hypericum). *Molecular Phylogenetics and Evolution 67*, 379-403.

Narayanan, K. B., & Sakthivel, N. (2011). Green synthesis of biogenic metal nanoparticles by terrestrial and aquatic phototrophic and heterotrophic eukaryotes and biocompatible agents. *Advances in Colloid and Interface Science 169*, 59-79.

Orčić, Dejan Z.; Mimica-Dukić, Neda M.; Francišković, Marina M.; Petrović, Slobodan S. and Jovin, Emilija. (2011). Antioxidant activity relationship of phenolic compoudns in *Hypericum perforatum* L. *Chemistry Central Journal 5*, 34.

Otari, S. V., R.M. Patil, S.J. Ghosh, N.D. Thorat, S.H. Pawar. (2015). Intracellular synthesis of silver nanoparticle by actinobacteria and its antimicrobial activity. *Spectrochimica Acta Part A: Molecular and Biomolecular Spectroscopy 136*, 1175-1180

Rajan, A., Kumari, M.M. & Philip, D. (2014). Shape tailored green synthesis and catalytic properties of gold nanocrystals. *Spectrochimica Acta Part A: Molecular and Biomolecular Spectroscopy 118*, 793-799.

Rajan, A., Rajan, A. R., & Philip, D. (2017). Elettaria cardamomum seed mediated rapid synthesis of gold nanoparticles and its biological activities. *OpenNano 2*, 1-8.

Rajeshkumar, S., Malarkodi, C., Vanaja, M., & Annadurai, G. (2016). Anticancer and enhanced antimicrobial activity of biosynthesizd silver nanoparticles against clinical pathogens. *Journal of Molecular Structure 1116*, 165-173.

Roy, E., Patra, S., Saha, S., Madhuri, R., & Sharma, P. K. (2015). Shape-specific silver nanoparticles prepared by microwave-assisted green synthesis using pomegranate juice for bacterial inactivation and removal. *RSC Advances 5*, 95433-95442.

Rusalepp, L., Raal, A., Püssa, T., & Mäeorg, U. (2017). Comparison of chemical composition of *Hypericum perforatum* and *H. maculatum* in Estonia. *Biochemical Systematics and Ecology 73*, 41-46.

Saha, K., Agasti, S. S., Kim, C., Li, X., & Rotello, V. M. (2012). Gold nanoparticles in chemical and biological sensing. *Chemical Reviews 112*, 2739-2779.

Singleton, V. L., & Rossi, J. A. (1965). Colorimetry of total phenolics with phosphomolybdic-phosphotungstic acid reagents. *American journal of Enology and Viticulture 16*, 144-158.

Taraj, K., Cikoa, L., Malollaria, I., Andonia A., Yllib, F., Yllia, A., Plakub, E., Llupac, J., Borshi, X. (2019). Eco-extraction of essential oil from albanian *Hypericum perforatum* L. and characterization by spectroscopy techniques. *Journal of Environmental Protection and Ecology 20*, 188-195

Vazquez-Muñoz, R., & Huerta-Saquero, A. Nanomateriales con actividad microbicida: una alternativa al uso de antibióticos. *Mundo Nano. Revista Interdisciplinaria en Nanociencia y Nanotecnología 7*, 37 - 47.

Wagner, H., & Bladt, S. (1994). Pharmaceutical quality of *Hypericum perforatum* extracts. *Journal of Geriatric Psychiatry and Neurology 7*, 65-68 .

Wang, L., Hu, C., & Shao, L. (2017). The antimicrobial activity of nanoparticles: present situation and prospects for the future. *International Journal of Nanomedicine 12*, 1227.

Zhang, X. (2015). Gold nanoparticles: recent advances in the biomedical applications. *Cell Biochemistry and Biophysics 72*, 771-775.